

Performance of Gaussian Mixture Model Classifiers on Embedded Feature Spaces

Jeremy Chopin, Rozenn Dahyot*

^aComputer Science Department, Maynooth University, Maynooth, Ireland

Abstract

Data embeddings with CLIP [15] and ImageBind [8] provide powerful features for the analysis of multimedia and/or multimodal data. We assess their performance here for classification using a Gaussian Mixture models (GMMs) based layer as an alternative to the standard Softmax layer. GMMs based classifiers have recently been shown to have interesting performances as part of deep learning pipelines trained end-to-end [9]. Our first contribution is to investigate GMM based classification performance taking advantage of the embedded spaces CLIP [15] and ImageBind [8]. Our second contribution is in proposing our own GMM based classifier with a lower parameters count than previously proposed [9]. Our findings are, that in most cases, on these tested embedded spaces, one gaussian component in the GMMs is often enough for capturing each class, and we hypothesize that this may be due to the contrastive loss used for training these embedded spaces that naturally concentrates features together for each class. We also observed that ImageBind [8] often provides better performance than CLIP [15] for classification of image datasets even when these embedded spaces are compressed using PCA.

Keywords: Classification, Gaussian mixtures, Deep Neural Networks

1. Introduction

Gaussian mixture models (GMMs) are well known powerful parametric probability density functions, popular for modelling likelihoods for classes of interest in D dimensional feature spaces. These likelihood-GMMs together with their respective class priors can then be used for defining a Bayes Classifier. Hayashi and Uchida [9] have proposed the Sparse Discriminative Gaussian mixture (SDGM) layer and have compared it with Softmax classifier as part of several deep learning pipelines that are trained end-to-end with the classifier layer. Here we first evaluate SDGM on data embeddings computed with CLIP [15] and ImageBind [8].

SDGM [9] estimates GMMs with the choice of full covariance matrices (with $D(D - 1)/2$ parameters for each covariance; the resulting classifier is noted SDGM-F) and lower dimensional diagonal covariance matrices (with D parameters for each covariance; the resulting classifier is noted SDGM-D). We propose our own deep neural network layer called Deep Gaussian Mixture Model Classifier (DGMMC) that similarly is able to fit both GMMs as likelihoods and estimate their corresponding class priors, for performing Bayesian classification. DGMMC¹ has a different implementation to SDGM² and it also allows to use spherical covariance matrices (noted DGMMC-S) that has a much lower number of parameters (only 1 parameter per covariance matrices). Our new layer for classification DGMMC is presented in Section 3 and its complexity is compared to SDGM in Section 4.

As part of a classifier layer, a linear operation can be learnt for reducing (or extending) the dimensionality D of the embedding space before fitting GMMs. We explore several strategies in Section 5 for that linear operation when we benchmark our approach for classification on several image datasets to demonstrate DGMMC performance. Overall our findings are that accuracies are better on CLIP and ImageBind than with reported end to end pipelines [9], that ImageBind performs better than CLIP, and the number of Gaussians required in the GMMs can be kept small (e.g $G = 1$) on these embedded spaces. A summary table of our accuracy results is shown Tab. 1. We start next by providing an overview of the relevant literature.

MNIST	CIFAR10	CIFAR100	ImageNet	ESC50
99.3	98.8	91.2	84.1	87
DGMMC-S Tab.4	DGMMC-S Tab. 5	DGMMC-S Tab.4	DGMMC-S Tab.4	SDGM-D Tab.7
99.14*	89.54*	78.68*	67.6*	66.9°

Table 1: For the tested datasets (top row), **our best classification accuracies obtained with ImageBind** are reported (second row) with the names of the classifier (3rd row). The corresponding Tables where these results are extracted from, are indicated in the 4th row. All models are with $G = 1$ except for CIFAR10 and ESC50 where $G = 2$. For comparison, the reported best accuracies from [9]* (with an end-to-end pipeline using SDGM-F) and [8]° (zero shot classification) are shown on the bottom line.

2. Related works

2.1. Classification of images

Convolutional Neural Networks (CNNs) have demonstrated excellent performance for image classification and some recent

*Corresponding author: Rozenn Dahyot

Email address: Rozenn.Dahyot@mu.ie (Rozenn Dahyot)

¹DGMMC code provided at <https://github.com/CVMLmu/DGMMC/>.

²SDGM https://github.com/HideakiHayashi/SDGM_ICLR2021/.

efforts have focused on efficient computing of convolution layers [17] or learning activation functions that follows convolution operations [2]. More recently Transformers (ViTs) [6] have been proposed as an alternative to CNNs, that are able to take advantage of long range spatial correlation in images that are often missed when using CNNs. Currently, Softmax is used as the final layer in both CNNs and Vision Transformers (ViTs) for classification decision [2, 6, 17].

2.2. Classifiers and GMMs

Classifiers that are based on a Softmax layer have achieved remarkable performance for the image classification task. However, as summarized in the work of Liang et al [13], these classifiers have shortcomings. First, the decision boundaries are learnt between the C classes in the D -dimensional feature space but does not learn the intrinsic class characteristics and can be limited for generalizing on unseen data. Secondly, each class c is captured by a single projection shifted with a bias hence the implicit assumption of the unimodality of each class in the feature space. Finally, the prediction score of a class is unreliable for uncertainty modelling and is only used for its comparative value against other classes. classifiers can focus instead on learning the joint data distribution using for instance Gaussian Mixture models (GMMs) [13]. Indeed GMMs are powerful probabilistic models that estimate any density provided there is enough Gaussian components in the mixture [10]. GMMs have been used for image classification. For instance Wan et al [18] train their GMMs using the Expectation-Maximization (EM) algorithm with an additional criteria to choose the adequate number of Gaussian components in the GMMs. GMMs have also been used in the context of deep learning for image classification: for instance Celarek et al [3] propose a convolutional neural network layer processing a GMM (input) into another GMM (output) with learnable filters also defined as GMMs. However their architecture uses Softmax for generating class scores [3]. Zhang et al. [19] used a Gaussian mixture as a measure of the attention in Transformer Model for Natural Language Processing (NLP) tasks. Gepperth et al [7] proposed to fit GMMs using a Stochastic Gradient Descent instead of the EM algorithm and obtained remarkable results, encouraging us to include the estimation of the parameters of the GMMs as parts of the neural network model.

Liang et al [13] recently proposed the use of GMMs as a classifier and obtain competitive results for semantic segmentation on benchmark datasets. Their model is composed of a feature extractor and a classifier based on GMMs trained with an hybrid training, where the feature extractor is trained using a Softmax layer (discriminative classifier) and the GMMs of the classifier are trained using a modified EM Algorithm based on optimal transport [5].

Closely related to our work is the sparse discriminative Gaussian mixture (SDGM) layer [9] that has been proposed for classification and compared favorably with traditional classification techniques and Softmax layer on synthetic and image datasets. In Section 3, we propose likewise a classifier layer using GMMs where all parameters of the Neural Networks and of GMM classifier layer (i.e. means, covariance matrix and weights) can

be optimized end-to-end using standard optimisation used with deep neural networks.

2.3. Embedding spaces with contrastive learning

Contrastive learning aims at learning a representation such that certain pairs of inputs (positive pairs), are close in the embedding space, while other pairs of inputs (negative pairs) are far apart [1]. In contrastive-language image pretraining (CLIP) [15], a positive pair consists of an image and its corresponding text caption, that are processed with two separate functions (one for each modality) and these positive pairs are close inputs to the embedding space. ImageBind [8] extends this idea using positive pairs of an image with additional modalities including for instance text (like CLIP), audio and other type of images (e.g. depth, thermal). The images in the pairs ((image, other data)) is sufficient to bind the data modalities together [8]. Separate transformers are used to process each modalities, for instance ViTs [6] are used to process image modalities for both (CLIP) [15] and ImageBind [8]. In this paper we have used the two pre-trained transformers provided by CLIP and ImageBind for processing image datasets, hence creating powerful features for our classifiers. In addition we also show classification results on an audio dataset that has been processed with the ImageBind pre-trained audio function (cf. Sec. 5).

3. DGMMC: Deep Gaussian Mixture Model Classifier

In the following, we denote x a feature (e.g. computed with CLIP or ImageBind) to classify into C classes. The likelihood $p(x|c)$ for class $c = 1, \dots, C$ is modelled as a GMM with G components (Gaussians).

3.1. GMMs: Gaussian Mixture Models

The posterior probabilities $\{p(c|x)\}_{c=1,\dots,C}$ are represented with Gaussian Mixture Models, and features extracted from images are used as inputs for our GMMs classifier. The goal here is to model the joint distribution $p(x, c)$ by estimating both the class-specific distribution $p(x|c)$ and the prior probability of each class $p(c)$. Then using Bayes rules we can estimate the posterior probabilities as:

$$p(c|x) = \frac{p(x|c) p(c)}{\sum_{c'=1}^C p(x|c') p(c')} \quad (1)$$

where C is the number of classes considered. The GMM $p(x|c)$ is composed of multivariate Gaussians for embedded features $x \in \mathbb{R}^D$ noted:

$$p(x|c) = \sum_{i=1}^{k^c} \omega_i^c \phi(x|\mu_i^c, \Sigma_i^c) \quad (2)$$

where k^c is the number of Gaussian components in the mixture for the class c . ϕ is the multivariate Gaussian distribution and $\omega_i^c, \mu_i^c, \Sigma_i^c$ are respectively the weights, the means and the covariance matrix of the Gaussian component i in the mixture for the class c . To limit the complexity of estimating $D \times D$ covariance matrices $\{\Sigma_i^c\}$ having $\frac{D \times (D+1)}{2}$ parameters, spherical

Gaussian mixtures are considered instead [7]: where $\Sigma_i^c = b_i^c \mathbf{I}_D$ with bandwidth b_i^c and identity matrix \mathbf{I}_D . In this case, Equation 1 becomes:

$$p(c|x) = \frac{p(c) \sum_{i=1}^G \omega_i^c \phi(x|\mu_i^c, b_i^c \mathbf{I}_D)}{\sum_{c'=1}^C [p(c') \sum_{i=1}^G \omega_i^{c'} \phi(x|\mu_i^{c'}, b_i^{c'} \mathbf{I}_D)]} \quad (3)$$

with the additional constraint for that all GMMs have the same number of components: $k^c = G, \forall c \in \{1, \dots, C\}$.

3.2. Deep Gaussian Mixture Model

Our classifier is trained as part of a deep neural network using Stochastic Gradient Descent (SGD). Based on equation 3, the following tensors are defined as parameters to estimate in our layer:

- $\mathbf{P} \in \mathbb{R}^C$ stores the prior $p(c)$ of each class and it has the following constraint:

$$\left(\sum_{c=1}^C P_c = 1 \right) \quad \wedge \quad (P_c \geq 0, \forall c = 1, \dots, C) \quad (4)$$

- $\mathbf{W} \in \mathbb{R}^{C \times G}$ is capturing the positive weights of the Gaussian components for all C classes GMMs, and has the following constraint:

$$(\forall c \in C, \mathbf{W} \mathbf{1}_G = \mathbf{1}_C) \quad \wedge \quad (W_{i,j} \geq 0, \forall (i, j)) \quad (5)$$

with the notation $\mathbf{1}_G$ (resp. $\mathbf{1}_C$) for a vector of ones in \mathbb{R}^G (resp. in \mathbb{R}^C).

- $\mathbf{M} \in \mathbb{R}^{C \times G \times D}$ is the tensor collecting all the mean vectors in \mathbb{R}^D .
- Finally, the tensor $\mathbf{B} \in \mathbb{R}^{C \times G}$ encodes the positive bandwidths with the constraint $B_{i,j} > 0, \forall (i, j)$.

The softmax operation is used to enforce the constraints on parameter tensors \mathbf{P} and \mathbf{W} . For the bandwidths \mathbf{B} , these are clamped with a minimal value set to be close to zero ($1e-6$). Our classifier is trained using SGD optimizer [7] with the cross-entropy loss.

3.3. Computational complexity DGMMC

Table 2 summarizes the number of parameters in our proposed models DGMMCs. The main gain that can be achieved is in choosing spherical covariance matrices and consequently in this paper we focus on our low parameter model DGMMC-S to compare with SDGM-F and SDGM-D proposed by Hayashi and Uchida [9]. The total number of parameters P_{rm} to estimate in our classifier layer DGMMC-S can be calculated as follow:

$$P_{rm} = C \times (G \times (D + 2) + 1) \quad (6)$$

3.4. Remarks

We have used one GMM per class where each GMM is composed of a number of G Gaussian components in the feature space of dimension D as in [9, 13].

	$\{\mu_i^c\}$	$\{p(c)\}^*$	$\{\omega_i^c\}^{**}$	$\{\Sigma_i^c\}$
DGMMC-F	DGC	C	GC	D^2CG
DGMMC-D	DGC	C	GC	DCG
DGMMC-S	DGC	C	GC	CG

Table 2: Number of learnt parameters for DGMMC classifiers with *formula for the number of classes $C \geq 2$ (task of classification in at least 2 classes) and **formula for the number of Gaussian components $G \geq 2$ (for $G = 1$, there is no learnt parameter as $\omega^c = 1, \forall c$) in a feature space of dimension D .

3.4.1. About GMMSeg [13]

Some key differences exist with Liang et al [13]’s formalism. First, Liang et al [13] use fixed uniform priors $p(c) = \frac{1}{C}$ for each class while our model is estimating those priors during the training. Secondly, Liang et al [13] couple the EM optimization for learning GMMs with learning features, while the parameters of the GMMs are learnable parameters of our model. Thirdly the weights of the Gaussian components have been chosen equiprobable $\omega = \frac{1}{G}$ by Liang et al [13] (to ease estimation with the EM algorithm and forcing it to split the N_c training samples evenly across the G Gaussians), but these weights are estimated instead in our model.

3.4.2. Comparison to SDGM [9]

Instead of using means and covariances as parameters of Gaussians, SDGM [9] uses a tensor \mathbf{w} as parameter of a multivariate Gaussian of the form $\propto \exp(\mathbf{w}^T \phi)$ where tensor ϕ captures a second order polynomial form of the input feature. Both \mathbf{w} and ϕ are vectors of higher dimension $H = 1 + D(D + 3)/2$ than the feature space dimension D , and their GMM layer is more akin to a polynomial neural network layer [4]. The Elbo loss is used for optimisation instead of the cross entropy.

3.4.3. Dimensionality reduction

In Section 5, we investigate several strategies for reducing the dimension D of the features in the CLIP and ImageBind embedding spaces. One well know strategy is in using a standard learnt linear layer reducing the dimension D to dimension d before the classifier layer. Note that for a Softmax classifier layer, the resulting dimension d needs to be the number of classes $d = C$. However here using GMM-based classifiers, d can be set as any integer $d \in \mathbb{N}$. In our experiments we mainly test for $d = D, d = C$ and some selected lower dimensions.

4. Computational complexity DGMMC-S Vs SDGM

Table 3 provides the number of trainable parameters for several of our tested DGMMC-S classifiers (bottom two rows, #), and, for comparison, also provides the number parameters for models SDGM-F as ratio:

$$\times \text{SDGM-F}(G, d) = \frac{\# \text{SDGM-F}(G, d)}{\# \text{DGMMC-S}(G, d)} \quad (7)$$

and similarly for SDGM-D:

$$\times \text{SDGM-D}(G, d) = \frac{\# \text{SDGM-D}(G, d)}{\# \text{DGMMC-S}(G, d)} \quad (8)$$

		$C = 10$		$C = 100$		$C = 1000$			
		$d = 2$	$d = 10$	$d = 32$	$d = 100$	$d = 128$	$d = 768$	$d = 1000$	$d = 1024$
×SDGM-F Eq. (7)	$G=1$	2.75×	10.92×	32.97×	101×	129×	769×	1001×	1025×
	$G=2$	2.44×	10.48×	32.49×	100.5×	128.5×	768.5×	1000.5×	1024.5×
×SDGM-D Eq. (8)	$G=1$	2.25×	3.42×	3.79×	3.93×	3.95×	3.99×	3.99×	3.99×
	$G=2$	2×	3.28×	3.74×	3.91×	3.93×	3.99×	3.99×	3.99×
# DGMMC-S	$G=1$	#40	#120	#3400	#10200	#130000	#770000	#1002000	#1026000
	$G=2$	#90	#250	#6900	#20500	#261000	#1541000	#2005000	#2053000

Table 3: Ratios of the number of parameters in SDGM-F and SDGM-D w.r.t. our model DGMMC-S. The numbers of parameters in DGMMC-S are provided in the bottom row (see Sec. 4). The choices for dimension d , number of classes C and number of Gaussian components $G = \{1, 2\}$ correspond to the classification accuracy results reported in the next Section 5.

where “# M” denotes “number of parameters for classifier M”. From Tab. 3, we note:

- the number of parameters for SDGM-F is about d times the number of parameters of our model DGMMC-S:

$$\# \text{SDGM-F} \simeq d \times \# \text{DGMMC-S}$$

- For SDGM-D, we note its number of parameters about 4 times the number of parameters of our model DGMMC-S:

$$\# \text{SDGM-D} \simeq 4 \times \# \text{DGMMC-S}$$

5. Classification accuracy on CLIP and ImageBind

We assess the classification accuracy of our classifier DGMMC-S in comparison to SDGM-F Vs SDGM-D classifiers, with or without linear layer.

Datasets. For this experience we are considering the MNIST ($C = 10$), CIFAR10 ($C = 10$), CIFAR100 ($C = 100$) and ImageNet ($C = 1000$) datasets [12, 11, 16] for the task of image classification with both CLIP and ImageBind as feature extractor. The ESC-50 ($C = 50$) dataset [14] is also tested using ImageBind as the feature extractor.

Embedded spaces. For all datasets we compute their CLIP features [15] (except audio dataset ESC-50) and ImageBind features [8] (all datasets). Unlike CLIP, ImageBind is able to compute features for other modalities (including audio) than images, hence classification accuracy results are also reported with the audio dataset ESC-50 ($C = 50$) with ImageBind features only. Both CLIP and ImageBind have been provided with their trained weights and all datasets used in this paper have their CLIP/ImageBind features pre-computed and saved locally for efficiency. CLIP provides $D = 768$ features and ImageBind provides $D = 1024$ features. When a linear layer is used before the classifier to reduce the dimension D to d , several dimensions d of feature spaces are tested.

Experiments. Acting as a baseline with $G = 1$, the first experiment (Sec. 5.1) performs classification directly on the embedding feature spaces without linear transformation (or equivalently the linear transformation matrix is set to the identity matrix). The second experiment (Sec. 5.2) learns a linear layer in

addition to the parameters of the classifiers, while the last experiment proposes to use principal components computed with PCA instead of learning a linear layer (Sec. 5.3).

5.1. Classification on embedded feature spaces with $G = 1$

DGMMC-S, SDGM-F and SDGM-D classifier performances are compared here in the simpler case where only one $G = 1$ Gaussian is used to represent each class.

Pipeline summary. The data is transformed as follow:

$$\text{Data} \rightarrow \underbrace{\text{feature: } \mathbf{x} \in \mathbb{R}^D}_{\text{CLIP or ImageBind}} \rightarrow \mathbf{x} = \mathbf{y} \rightarrow \underbrace{\text{Classifier}(\mathbf{y})}_{\text{learnt}} \quad (9)$$

Training Protocol. All classifiers, DGMMC-S, SDGM-F and SDGM-D, are trained using SGD optimizer with momentum (set to 0.9) and Nesterov acceleration. The initial learning rate is set at $1e - 3$ and decreases to $1e - 4$ using a cosine annealing scheduler over 30 epochs.

Results. Table 4 shows the classification mean accuracy with standard deviation (computed over 3 runs) obtained with DGMMC-S, SDGM-F and SDGM-D. First, ImageBind features perform best on all datasets in comparison to CLIP features. With ImageBind, our proposed classifier DGMMC-S performs the best in comparison to SDGM-F and SDGM-D that use more complex covariance matrices (at the exception of audio dataset ESC-50 where SDGM-D performs best). On the other hand, on CLIP feature space, SDGM classifiers perform better than the simpler DGMMC-S. Note that SDGM-F could not be run for ImageNet for the machine used for our experiments: this classifier has too many parameters (SDGM-F has about D times more parameters than DGMMC-S, c.f. Tab. 3 with $G = 1$, $C = 1000$, $G = 1$ and $d = D = 768$ (CLIP) and $d = D = 1024$ (ImageBind)).

5.2. Classifiers with a learnt transformation

DGMMC-S, SDGM-F and SDGM-D classifier performances are compared here with using a learnt linear transformation for reducing the dimensionality. Additionally we test both $G = 1$ and $G = 2$ Gaussian components as part of the GMMs representing each class. In this experience, we are considering a linear layer with bias in order to change the D -dimensional feature space into a d -dimensional feature space. This operation

	CLIP ($d = D = 768$)		
Datasets	SDGM-F	SDGM-D	DGMMC-S
MNIST	98.9 (0.1)	98.1 (0.1)	86.7 (0.6)
CIFAR10	97.8 (0.003)	97.5 (0.04)	88.7 (2.9)
CIFAR100	85.9 (0.2)	84.1 (0.3)	72.1 (1.0)
ImageNet	x	80.1	71.6

	ImageBind ($d = D = 1024$)		
Datasets	SDGM-F	SDGM-D	DGMMC-S
MNIST	94.4 (1e-3)	93.4 (0.1)	99.3 (0.1)
CIFAR10	98.3 (0.01)	98.1 (0.02)	98.7 (4e-3)
CIFAR100	82.4 (0.2)	79.5 (0.6)	91.2 (0.02)
ImageNet	x	59.8	84.1
ESC-50	81 (2)	82.3 (2.3)	57.3 (8.9)

Table 4: Accuracy % (mean and standard deviation computed over 3 runs, excluding ImageNet) for classification with GMM based classifiers ($G = 1$) (cf. Sec. 5.1, pipeline (9)). Bold highlight best accuracy with underline for second best accuracy.

allows to reduce the number of features used by the classifiers, hence limiting of the number of trainable parameters to learn during the training even if we need to consider the parameters of the linear layer that now also need to be trained.

Pipeline summary. The data is transformed as follow:

$$\text{Data} \rightarrow \underbrace{\text{feature: } \mathbf{x} \in \mathbb{R}^D}_{\text{CLIP or ImageBind}} \rightarrow \underbrace{\text{lin}(\mathbf{x}) = \mathbf{y} \in \mathbb{R}^d}_{\text{learnt}} \rightarrow \text{Classifier}(\mathbf{y}) \quad (10)$$

Training Protocol. The models are trained using and SGD optimizer with momentum (set to 0.9) and Nesterov acceleration. The initial learning rate is set at $1e-3$ and decreases to $1e-4$ using a cosine annealing scheduler over 50 epochs.

Results. Table 5 provides the averaged accuracy results and standard deviation (over 5 runs) on the CIFAR10 and CIFAR100 datasets. Choosing $G = 2$ Gaussian components sometimes improves slightly classifier’s performances (DGMMC-S and SDGM-D): two Gaussians components may be helpful in compensating the simplicity of one spherical or diagonal Gaussian representing a class. Best performances are again observed for ImageBind feature space in comparison to CLIP. A higher dimension d allows to improve all results for CIFAR10/100 (Tab. 5) and most classifiers accuracies on ImageNet dataset (Tab. 6) and audio dataset ESC-50 (Tab. 7).

Remarks. Reducing the number of features using a linear layer allows to limit the number of trainable parameters in the classifiers and we observe that accuracy results with the linear layer compares well in comparison to using features directly provided by the pretrained embedding space. However, the linear layer is dependent of the hyperparameter d , which need to be set arbitrarily. We propose next to replace this linear layer by a PCA decomposition in order to reduce the feature space to a suitable d -dimensional eigenspace for performing classification.

5.3. Using PCA as linear transformation

The linear layer is now replaced by computing the mean and the Principal Components using all training features (all classes), and retaining the ones with the highest eigenvalues for projection in a reduced d -dimensional space.

Pipeline summary. The data is transformed as follow:

$$\text{Data} \rightarrow \underbrace{\text{feature: } \mathbf{x} \in \mathbb{R}^D}_{\text{CLIP or ImageBind}} \rightarrow \underbrace{\text{lin}(\mathbf{x}) = \mathbf{y} \in \mathbb{R}^d}_{\text{PCA}} \rightarrow \underbrace{\text{Classifier}(\mathbf{y})}_{\text{learnt}} \quad (11)$$

Training Protocol. We replace the linear layer used in the previously (Sec. 5.2) to reduce the dimension space of the features by a PCA decomposition. The cumulative explained variance ratio (Eq. 12) can then be used to select the number d of eigenvectors capturing a reasonable chunk of the information:

$$\text{variance ratio}(d) = \frac{\sum_{j=1}^d \lambda_j}{\sum_{j=1}^D \lambda_j} \quad (12)$$

where D is the number of dimension in the embedded feature spaces ($D = 768$ for CLIP and $D = 1024$ for ImageBind), d represents the first d principal components and λ_j is the variance (eigenvalue) of the data around the j -th eigenvectors. Classifiers all use $G = 1$ Gaussian component per class.

Results. Fig. 1 shows the accuracy of the classifiers with respect to the explained variance for CIFAR100 (images) dataset and the ESC-50 (audio sounds) datasets. We note that ImageBind features again provide best result in comparison to CLIP features. For ESC-50 we note that accuracy falls when too many principal components are used (d high: principal components associated with lowest eigenvalues may capture noise not representative of the classes and inclusion of these dimensions impact negatively the performance of the classifiers. Tab. 8 shows the accuracy obtained for ImageNet dataset using 80% of the variance ratio.

6. Conclusions

Both ImageBind and CLIP features were trained using contrastive learning that may explain why, in practice, we did not notice major advantages in using more than one Gaussian component in the GMMs encoding the classes. Depending on the datasets and the embedding feature spaces, estimating full covariance matrices (with SDGM-F) provide the best results with CLIP, however simpler covariance matrices, diagonal (SDGM-D) and spherical (DGMMC-S) perform better with ImageBind and with less parameters. Occasionally having $G = 2$ Gaussian components in the GMMs may help DGMMC-S to perform as well as SDGM-F with $G = 1$. ImageBind embedded space has a higher dimensionality $D = 1024$ than CLIP $D = 768$ and ImageBind has shown to perform better than CLIP most of the time. Decreasing the D -dimensional embedded space using a PCA based linear transform to a lower d -dimensional one has also shown to be valuable in reducing complexity while

Model	G	$d = 2$	$d = 10$
<u>SDGM-F</u>	1	94.9 (0.4)	97.8 (0.1)
	2	94.4 (0.5)	97.8 (0.1)
SDGM-D	1	94.7 (0.3)	97.7 (0.02)
	2	94.5 (0.4)	97.7 (0.02)
DGMMC-S	1	91.9 (0.1)	97.8 (0.1)
	2	93.6 (0.3)	97.7 (0.1)

(a) CIFAR10-CLIP

Model	G	$d = 2$	$d = 10$
<u>SDGM-F</u>	1	94.4 (0.3)	98.8 (0.02)
	2	93.9 (0.3)	98.7 (0.02)
SDGM-D	1	94.5 (0.3)	98.5 (0.1)
	2	93.8 (0.7)	98.5 (0.1)
DGMMC-S	1	93.6 (1.5)	98.7 (0.1)
	2	95.0 (0.3)	98.8 (0.05)

(b) CIFAR10-ImageBind*

Model	G	$d = 32$	$d = 100$
SDGM-F	1	84.2 (0.4)	85.7 (0.1)
	2	84.1 (0.2)	85.6 (0.1)
<u>SDGM-D</u>	1	84.2 (0.3)	85.3 (0.1)
	2	84.2 (0.2)	85.5 (0.3)
DGMMC-S	1	81.5 (0.1)	84.3 (0.1)
	2	81.5 (0.1)	84.1 (0.3)

(c) CIFAR100-CLIP

Model	G	$d = 32$	$d = 100$
SDGM-F	1	89.0 (0.1)	90.5 (0.1)
	2	88.7 (0.1)	90.2 (0.1)
SDGM-D	1	81.6 (1.3)	83.4 (0.6)
	2	73.1 (2.0)	77.6 (0.3)
<u>DGMMC-S</u>	1	86.3 (0.3)	89.1 (0.5)
	2	86.6 (0.3)	89.7 (0.2)

(d) CIFAR100-ImageBind*

Table 5: Accuracy % (mean and standard deviation computed over 5 runs) for classification of datasets **CIFAR10** and **CIFAR100** (cf. Sec 5.2, pipeline (10)). Best model in bold with second best underlined (when equal accuracy, the model with the lowest number of parameters is ranked first), and overall best performing features indicated with *.

Model	G	$d = 128$	$d = 768$	$d = 1000$	$d = 1024$
<u>SDGM-F</u>	1	81.1	x	x	x
	2	81.3	x	x	x
SDGM-D	1	82.6	83.7	82.5	83.8
	2	82.6	83.7	82.4	83.8
DGMMC-S	1	69.6	79.1	79.9	79.5
	2	69.8	80.3	80.0	79.9

(a) ImageNet-CLIP*

Model	G	$d = 128$	$d = 768$	$d = 1000$	$d = 1024$
SDGM-F	1	83.5	x	x	x
	2	83.5	x	x	x
SDGM-D	1	80.9	81.9	82.3	82.4
	2	80.0	81.6	81.9	82.0
<u>DGMMC-S</u>	1	68.8	81.0	81.4	81.7
	2	69.3	82.6	83.0	83.1

(b) ImageNet-ImageBind

Table 6: Accuracy % for classification of dataset **ImageNet** (cf. Sec 5.2, pipeline (10)). Best model in bold with second best model underlined, and overall best performing features indicated with *.

Model	G	$d = 3$	$d = 50$	$d = 768$	$d = 1024$
<u>SDGM-F</u>	1	50 (4)	85 (2)	85 (2)	84 (1)
	2	49 (2)	84 (2)	84 (3)	82 (2)
SDGM-D	1	38 (2)	82 (2)	86 (3)	86 (2)
	2	36 (2)	83 (3)	86 (3)	87 (3)
DGMMC-S	1	37 (3)	81 (3)	77 (2)	73 (5)
	2	35 (2)	81 (2)	80 (6)	81 (3)

Table 7: Accuracy % (mean and standard deviation computed over 3 runs) for classification of dataset **ESC-50** with ImageBind features (cf. Sec. 5.2, pipeline (10)). Best model in bold with second best model underlined.

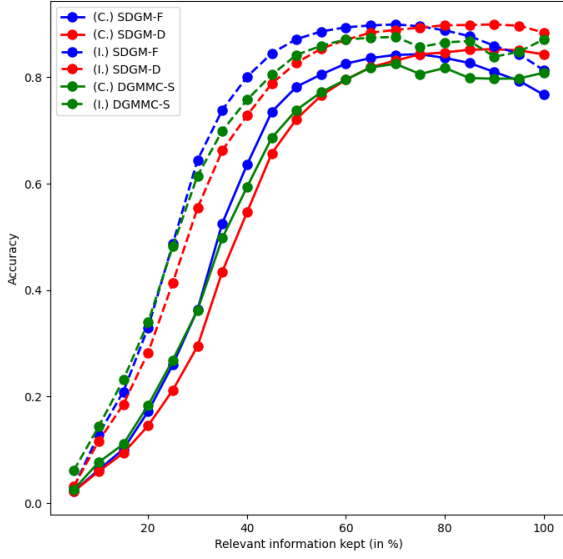
Embedding	CLIP	ImageBind
Model	$d = 221$	$d = 220$
SDGM-F	80.2	80.9
SDGM-D	81.4	82.0
DGMMC-S	76.9	79.3

Table 8: Accuracy on **ImageNet** using both DGMMC and SDGM classifiers when only using 80% of the variance ratio resulting in keeping the d most relevant PCA eigenvectors (cf. Sec. 5.3, pipeline (11)).

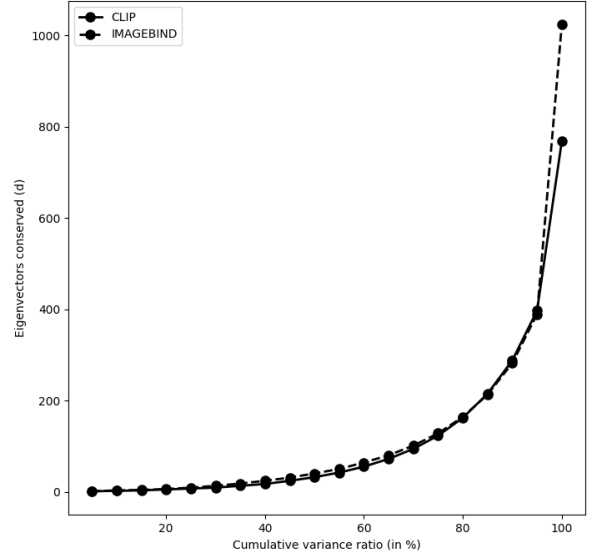
maintaining good performance. We have shown that the hyper-parameter choice of d can be selected conveniently using the cumulated variance ratio. We have extended SDGM classifiers by proposing to use spherical covariance matrices for Gaussians as part of our DGMMC-S classifier and all classifiers have been compared on the several datasets. Table 1 summarizes the best accuracy results: DGMMC-S has been shown to perform very well in practice on the ImageBind embedding space (without the need of linear layer preceding the classifier), and only the audio dataset is better classified when using a learnt linear layer with SDGM-D.

Acknowledgments

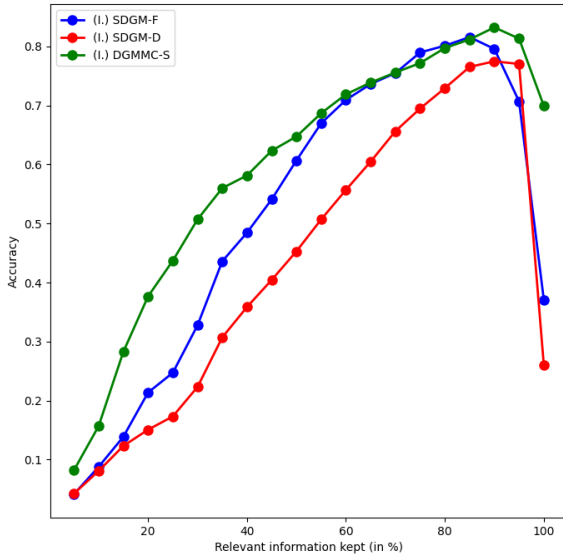
This research was conducted with the financial support of Science Foundation Ireland under Grant Agreement no. 13/RC/2106.P2 at ADAPT, the SFI Research Centre for AI-Driven Digital Content Technology, that is funded by Science Foundation Ireland through the SFI Research Centres Programme and is co-funded by the European Regional Development Fund. For the purpose of Open Access, the authors have



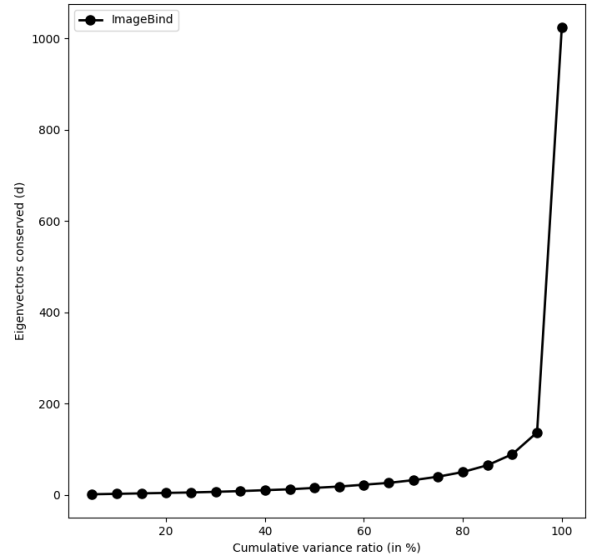
(a)



(b)



(c)



(d)

Figure 1: Evolution of the accuracy depending of the cumulative variance ratio kept (in %) after PCA decomposition on features provided by the pretrained embedding spaces CLIP (plain lines) and ImageBind (dashed lines). The results are provided for the **CIFAR100** dataset ((a) and (b)) and the **ESC-50** dataset ((c) and (d)) where 20 different percentages (from 5% to 100%) have been used to plot the curves (cf. Sec. 5.3).

applied a CC BY public copyright licence to any Author Accepted Manuscript version arising from this submission.

References

- [1] Bishop, C. M., & Bishop, H. (2024). *Deep Learning: Foundations and Concepts*. Springer International Publishing. URL: <http://dx.doi.org/10.1007/978-3-031-45468-4>. doi:10.1007/978-3-031-45468-4.
- [2] Bohra, P., Campos, J., Gupta, H., Aziznejad, S., & Unser, M. (2020). Learning activation functions in deep (spline) neural networks. *IEEE Open Journal of Signal Processing*, 1, 295–309. doi:10.1109/OJSP.2020.3039379.
- [3] Celarek, A., Hermosilla, P., Kerbl, B., Ropinski, T., & Wimmer, M. (2022). Gaussian mixture convolution networks. In *International Conference on Learning Representations*. URL: <https://openreview.net/forum?id=0xeka7Z7Hor>.
- [4] Chrysos, G. G., Moschoglou, S., Bouritsas, G., Deng, J., Panagakis, Y.,

- & Zafeiriou, S. (2022). Deep polynomial neural networks. *IEEE Transactions on Pattern Analysis and Machine Intelligence*, 44, 4021–4034. doi:10.1109/TPAMI.2021.3058891.
- [5] Cuturi, M. (2013). Sinkhorn distances: Lightspeed computation of optimal transport. In C. Burges, L. Bottou, M. Welling, Z. Ghahramani, & K. Weinberger (Eds.), *Advances in Neural Information Processing Systems*. Curran Associates, Inc. volume 26. URL: https://proceedings.neurips.cc/paper_files/paper/2013/file/af21d0c97db2e27e13572cbf59eb343d-Paper.pdf.
- [6] Dosovitskiy, A., Beyer, L., Kolesnikov, A., Weissenborn, D., Zhai, X., Unterthiner, T., Dehghani, M., Minderer, M., Heigold, G., Gelly, S., Uszkoreit, J., & Houshy, N. (2021). An image is worth 16x16 words: Transformers for image recognition at scale. In *International Conference on Learning Representations*. URL: <https://openreview.net/forum?id=YicbFdNTTy>.
- [7] Gepperth, A., & Pfülb, B. (2021). Gradient-based training of gaussian mixture models for high-dimensional streaming data. *Neural Process Letters*, 53, 4331–4348. doi:10.1007/s11063-021-10599-3.
- [8] Girdhar, R., El-Nouby, A., Liu, Z., Singh, M., Alwala, K. V., Joulin, A., & Misra, I. (2023). Imagebind: One embedding space to bind them all. In *Proceedings of the IEEE/CVF Conference on Computer Vision and Pattern Recognition (CVPR)* (pp. 15180–15190). URL: https://openaccess.thecvf.com/content/CVPR2023/papers/Girdhar_ImageBind_One_Embedding_Space_To_Bind_Them_All_CVPR_2023_paper.pdf.
- [9] Hayashi, H., & Uchida, S. (2021). A discriminative gaussian mixture model with sparsity. In *International Conference on Learning Representations*. URL: https://openreview.net/forum?id=-_Zp7r2-cGK.
- [10] Jian, B., & Vemuri, B. C. (2011). Robust point set registration using gaussian mixture models. *IEEE Transactions on Pattern Analysis and Machine Intelligence*, 33, 1633–1645. doi:10.1109/TPAMI.2010.223.
- [11] Krizhevsky, A. (2009). *Learning multiple layers of features from tiny images*. Technical Report Department of Computer Science, University of Toronto. URL: <https://www.cs.toronto.edu/~kriz/learning-features-2009-TR.pdf>.
- [12] Lecun, Y., Bottou, L., Bengio, Y., & Haffner, P. (1998). Gradient-based learning applied to document recognition. *Proceedings of the IEEE*, 86, 2278–2324. doi:10.1109/5.726791.
- [13] Liang, C., Wang, W., Miao, J., & Yang, Y. (2022). Gmmseg: Gaussian mixture based generative semantic segmentation models. In S. Koyejo, S. Mohamed, A. Agarwal, D. Belgrave, K. Cho, & A. Oh (Eds.), *Advances in Neural Information Processing Systems* (pp. 31360–31375). Curran Associates, Inc. volume 35. URL: https://proceedings.neurips.cc/paper_files/paper/2022/file/cb1c4782f159b55380b4584671c4fd88-Paper-Conference.pdf.
- [14] Piczak, K. J. (2015). ESC: Dataset for Environmental Sound Classification. In *Proceedings of the 23rd Annual ACM Conference on Multimedia* (pp. 1015–1018). ACM Press. URL: <http://dl.acm.org/citation.cfm?doid=2733373.2806390>. doi:10.1145/2733373.2806390.
- [15] Radford, A., Kim, J. W., Hallacy, C., Ramesh, A., Goh, G., Agarwal, S., Sastry, G., Askell, A., Mishkin, P., Clark, J., Krueger, G., & Sutskever, I. (2021). Learning transferable visual models from natural language supervision. In M. Meila, & T. Zhang (Eds.), *Proceedings of the 38th International Conference on Machine Learning Research*. PMLR volume 139 of *Proceedings of Machine Learning Research*. URL: <https://proceedings.mlr.press/v139/radford21a.html>.
- [16] Russakovsky, O., Deng, J., Su, H., Krause, J., Satheesh, S., Ma, S., Huang, Z., Karpathy, A., Khosla, A., Bernstein, M., Berg, A. C., & Fei-Fei, L. (2015). Imagenet large scale visual recognition challenge. *Int. J. Comput. Vision*, 115, 211–252. URL: <https://doi.org/10.1007/s11263-015-0816-y>. doi:10.1007/s11263-015-0816-y.
- [17] Ulicny, M., Krylov, V. A., & Dahyot, R. (2022). Harmonic convolutional networks based on discrete cosine transform. *Pattern Recognition*, 129, 1–12. URL: <https://arxiv.org/pdf/2001.06570.pdf>. doi:10.1016/j.patcog.2022.108707. ArXiv:2001.06570 Github: <https://github.com/matej-ulicny/harmonic-networks>.
- [18] Wan, H., Wang, H., Scotney, B., & Liu, J. (2019). A novel gaussian mixture model for classification. In *2019 IEEE International Conference on Systems, Man and Cybernetics (SMC)* (pp. 3298–3303). doi:10.1109/SMC.2019.8914215.
- [19] Zhang, S., & Feng, Y. (2021). Modeling concentrated cross-attention for neural machine translation with Gaussian mixture model. In M.-F. Moens, X. Huang, L. Specia, & S. W.-t. Yih (Eds.), *Findings of the Association for Computational Linguistics: EMNLP 2021* (pp. 1401–1411). Punta Cana, Dominican Republic: Association for Computational Linguistics. URL: <https://aclanthology.org/2021.findings-emnlp.121>. doi:10.18653/v1/2021.findings-emnlp.121.